# THERMAL IR REMOTE SENSING OF ATMOSPHERIC TRANSMITTANCE AND WATER VAPOR FROM AVHRR DATA

J. A. SOBRINO[1], Z.-L. LI[2], F. BECKER[2] and V. CASELLES[1]
[1] University of Valencia, Department of Thermodynamics. 50, Dr. Moliner, 46100 Burjassot (Spain)
[2] GSTS/LSIT/ENSPS, 7 rue de l'Université, 67000 Strasbourg (France)

## ABSTRACT

This paper describes how the spatial covariance ($\sigma_{45}$) and variance ($\sigma_{44}$) of image brightness temperature measured in Channels 4 (≈10.3-11.3 μm) and 5 (≈11.5-12.5 μm) of the Advanced Very High Resolution Radiometer (AVHRR) on board the NOAA-11 can be used to derive the atmospheric transmittance for each channel and the total column content of water vapor. The technique starts from the relationship exhibited between the ratio of atmospheric transmittances in the two channels of the split-window, and the observed variations of satellite brightness temperatures. This relationship is obtained under the condition that the atmosphere and the surface emissivity are unchanged over N neighboring pixels where the surface temperature changes. LOWTRAN-7 code was used to simulate remote sensing of atmospheric transmittance and water vapor over a wide range of situations and to test the accuracy of the method. The method was applied to AVHRR data over different regions and compared with other measurements (radiosounding or HIRS). Finally, it is shown, that the use of this information allows deriving a novel extension of the split-window technique which represents an improvement over the conventional algorithms for satellite-derived surface temperature.

**KEY WORDS:** Atmospheric transmittance, AVHRR, Split-Window, Water vapor.

## 1- INTRODUCTION

In order to improve the quality of remote-sensing data there is a need to estimate the atmospheric transmittance and/or the total water vapor from the image itself. In fact measurements of these parameters allow to improve the accuracy of remotely sensed surface temperature (ST) which is a necessity for many applications, notably agrometeorology, climatic and environmental studies. However the accurate determination of ST constitutes a difficult task. The principal sources of distortions are atmospheric attenuation and emission of thermal radiation and the non-black-body nature of the surface. Different techniques have been developed to eliminate these perturbations, the most popular being the split-window technique (McClain et al., 1985, etc). This technique takes advantage of the differential absorption in two adjacent spectral windows, centred at 10.8 μm and 12 μm for the AVHRR instrument, to correct for atmospheric effects and describes the surface temperature in terms of a simple linear combination of brightness temperatures $T_1$ and $T_2$ as measured in both thermal channels. $T_s=a_0+a_1T_1+a_2T_2$, where $T_s$ is the surface temperature measurement, and $a_0$, $a_1$, and $a_2$ are coefficients that have been chosen to minimize the error in the ST determination. With this point of view numerous studies have been made to determine the coefficients over the sea surface (McMillin, 1975; Deschamps an Phulpin, 1980; Barton et al., 1989) and land surface (Price, 1984; Becker and Li, 1990; Sobrino et al., 1991).

Although successful results have been obtained using these approaches, the algorithms given in these works do not respond to the stringent accuracy requirements for ocean (0.3 K) and land surface studies (1 K). In this direction Harris and Mason (1992), and Sobrino et al. (1994) demonstrated that the inclusion of the ratio of transmittances in Channels 4 and 5 of AVHRR, or, the total water vapor content in the algorithms permits the elimination of a significant quantity of error in the retrieval of SST and constitutes a large improvement over the currently used split-window algorithms. In recent years, numerous methods have been proposed to derive precipitable water and the channel transmittance ratio from satellite-based sounding radiometers such as the IRIS (Infra-red Interferometer Spectrometer) on board the NIMBUS-4 satellite (Prabhakara et al., 1979), the HIRS (High-resolution Infra-red Radiation Sounder) that is the infra-red part of TOVS (TIROS-N Operational Vertical Sounder) on board the NOAA satellite, the VISSR Atmospheric Sounder (VAS) on the GOES satellite (Chesters et al., 1983), etc. In practice, however, especially when the AVHRR data are the only available, it is more useful to apply methods that use the radiometric temperatures in two-infrared channels. Thus, Klesspies and McMillin (1990) obtain the ratio of transmittances from the channel brightness temperature differences by assuming that the atmosphere and surface emissivities in Channels 4 and 5 are invariant. Jedlovec (1990) proposes an extension of this technique that uses the ratio of the spatial variance of the channel brightness temperatures. Dalu (1987) and Schluessel (1989) presented other approaches that are based on the relationship exhibited between water vapor and the difference of brightness temperatures between the two infrared channels.

In this context, the objective of the present paper is to propose another technique that permits obtaining, for a cloud free situation, quantitative information on the atmospheric contribution to the radiance measured by a satellite borne sensor. This method, which is found insensitive to the values of channels emissivities, is practical because it obtains the atmospheric transmittance and the total water vapor content from satellite data alone. In this way it is possible to produce a novel extension to the standard split-window algorithm for better estimates of surface temperature from the brightness temperatures measured in Channels 4 and 5 of AVHRR.

## 2-PRINCIPLE OF METHOD

The radiance $I_i$ measured from space in channel i, for a cloud-free atmosphere under local thermodynamic equilibrium, may be written with good approximation as,

$$I_i = B_i(T_i) = \varepsilon_i B_i(T_s)\tau_i + R_{ati}\uparrow + (1-\varepsilon_i)R_{ati}\downarrow\tau_i \qquad (1)$$

In (1) all quantities refer to a spectral integration over the band width of channel i. $T_i$ is the corresponding brightness temperature of $I_i$, and $\varepsilon_i$ is the surface emissivity. $B_i(T_s)$ is the radiance which would be measured if the surface were a blackbody with the surface temperature $T_s$, $\tau_i$ is the total transmittance of the atmosphere, $R_{ati}\uparrow$ is the upwelling atmospheric radiance, and $R_{ati}\downarrow$ is the downwelling atmospheric radiance. The first term on the right-hand side is the radiation emitted by the surface that is attenuated by the atmosphere. The second term is the upwelling radiation emitted by the atmosphere towards the sensor and the third term is the downwelling radiation emitted by the atmosphere that reaches the earth's surface and then is reflected towards the sensor.

Under the condition that the atmosphere is unchanged over the neighboring points where the surface temperature changes, and considering adjacent pixels that does not present a large difference in the emissivity values; i.e.: sea and sand, (Sobrino et al., 1994), the variation of radiance measured from space in channel i due to the change of surface temperature ($\Delta T_s = T_{s1} - T_{so}$), can be expressed from Eq. (1) as

$$\Delta I_i = [B_i(T_{i1}) - B_i(T_{io})] = \varepsilon_i [B_i(T_{s1}) - B_i(T_{so})]\tau_i \qquad (2)$$

where $T_{i1}$ and $T_{io}$ are the brightness temperatures for the two conditions. If we expand the radiance $B_i(T)$ to first order approximation about its mean temperature $T_o$, in the form $B_i(T) = B_i(T_o) + (T-T_o)\frac{\partial B_i(T_0)}{\partial T}$, then Eq. (2) becomes

$$(T_{i1} - T_{io}) = \varepsilon_i (T_{s1} - T_{so})\tau_i \qquad (3)$$

Similarily, for the measurements in channel j, we have

$$(T_{j1} - T_{jo}) = \varepsilon_j (T_{s1} - T_{jo})\tau_j \qquad (4)$$

Dividing (4) by (3) gives

$$(T_{i1} - T_{io}) * \frac{\tau_j\varepsilon_j}{\tau_i\varepsilon_i} = T_{j1} - T_{jo} \qquad (5)$$

If the assumptions made above hold, for instance over N neighbouring pixels, then, by least-squares analysis of Eq. (5), the ratio of $\tau_j\varepsilon_j$ to $\tau_i\varepsilon_i$ can be obtained as

$$\frac{\tau_j}{\tau_i}\frac{\varepsilon_j}{\varepsilon_i} = \frac{\sum_{k=1}^{N}(T_{ik} - T_{io})(T_{jk} - T_{jo})}{\sum_{k=1}^{N}(T_{ik} - T_{io})^2} \qquad (6)$$

If emissivity in Channel 4 is equal to that in Channel 5 at a scale of an AVHRR pixel (this might be a good approximation for most surfaces) and if we define $R_{54}$ as

$$R_{54} = \frac{\sum_{k=1}^{N}(T_{4k} - T_{4o})(T_{5k} - T_{5o})}{\sum_{k=1}^{N}(T_{4k} - T_{4o})^2} \quad (7)$$

then Eq.(6) reduces to

$$\frac{\tau_5}{\tau_4} = R_{54} \quad (8)$$

where $\tau_4$ and $\tau_5$, are the total atmospheric transmittances in Channels 4 and 5 of the AVHRR/2 and where the numerator and denominator on the right-hand side of Eqn. (7) represent, respectively, the covariance and the variance of brightness temperatures directly measured by the satellite in channels 4 and 5, with $T_{4o}$ and $T_{5o}$ being two temperatures of reference, this could be the mean temperature of the pixels considered in each channel or the temperature of a single pixel.

**2.1. Evaluation of Total Transmittance**

Another significant application of this technique consists in obtaining the atmospheric transmittance. Thus, assuming that the total transmittance $\tau_k$ (k=4, 5) for channel k can be expressed as (Harris and Mason, 1992):

$$\tau_k = \tau_{kWater} * \tau_{kGas} \quad (9)$$

where $\tau_{kWater}$ and $\tau_{kGas}$ are respectively the total water transmittance and the total transmittance due to the other gases (for exemple, $O_3$, $CO_2$, $N_2$, $N_{20}$, $CH_4$ etc.). They are given by

$$\tau_{kWater} = \mathrm{Exp}(-A_k W_{Water} / \cos\theta) \quad (10a)$$

$$\tau_{kGas} = \mathrm{Exp}(-G_k W_{Gas} / \cos\theta) \quad (10b)$$

in which $\theta$ is the angle of observation; $A_k$ and $G_k$ are the band-average absorption coefficents in channel k, assumed to be independent of atmospheric temperature, for water vapor and other gases respectively; and $W_{water}$ and $W_{Gas}$ are respectively the total effective contents of water vapor and other gases.

Now, inserting Eq. (9) with Eqs.(10a) and (10b) into Eq. (8), one gets:

$$R_{54} = \mathrm{Exp}\frac{-(G_5 - G_4)*W_{Gas}}{\cos\theta} * \mathrm{Exp}\frac{-(A_5 - A_4)*W_{Water}}{\cos\theta} \quad (11)$$

and

$$\tau_4 = A*R_{54}^{B} \quad (12a)$$

$$\tau_5 = A*R_{54}^{(B+1)} \quad (12b)$$

with $A = \mathrm{Exp}(\frac{G_5 - CG_4}{C - 1} * \frac{W_{Gas}}{\cos\theta})$, $B = \frac{1}{C-1}$, and $C = \frac{A_5}{A_4}$

The importance of Eqs. (12a) and (12b) lies in that they give a method to obtain the actual atmospheric transmittance with only the brightness temperatures measured by the satellite, through $R_{54}$.

**2.2. Evaluation of Total Water Content W**

Water vapor in the atmosphere is an important constituent because it plays a significante role in the absorption and emission of radiative energy. Measurements of this constituent is important to increase the understanding of the biosphere-atmosphere interactions, the energy budget, and for monitoring climate change due to the

greenhouse gases (Kaufman and Gao, 1992). We can also retrieve the total water content in the vertical column, $W_{water}$, from Eq. (11), which reads

$$W_{Water} = \frac{-(G_5 - G_4)}{A_5 - A_4} * W_{Gas} - \frac{1}{A_5 - A_4} * \cos\theta \ln R_{54} \quad (13)$$

## 3- RESULTS

### 3.1. Application to simulated data

The validity of the modeled transmittances, Eqs. (12a) and (12b) and total water vapor, Eq. (13)), over the range of the adopted assumptions, particularly the lack of inclusion of the emissivity effect, has been checked from simulated AVHRR Channels 4 and 5 of NOAA-11 brightness temperature data. These data were calculated using the LOWTRAN-7 code (Kneizys et al., 1988) with the appropriate channel filter functions. Atmospheric profile input data were obtained from a set of 60 marine radiosoundings extracted from the TOVS initial guess retrieval (TIGR) (Scott and Chedin, 1981). These set of profiles cover a large range of temperature and moisture conditions. The calculation includes the effects of water vapor, molecular nitrogen, and the uniformly mixed gases ($CO_2$, $N_2O$, $O_3$, CO and $CH_4$). Three observation angles (0°, 23° and 46°), five surface temperatures, T-5, T, T+5, T+10, and T+20, (T is the first boundary layer temperature of the atmosphere) and 45 different combinations of Channels 4 and 5 emissivities ($\varepsilon_4$ and $\varepsilon_5$ ranging from 0.90 to 1.00 and five values of the emissivity differences, $\Delta\varepsilon=\varepsilon_4-\varepsilon_5$, ranging from -0.02 to 0.02) were also considered for each radiosounding. From these simulations we have constructed Figure 1, which corroborates the correlation existing between the transmittances and the right-hand side of Eq. (8). We find A=0.98 and B=1.90, and therefore,

$$\tau_4 = 0.98 \left(\frac{\sigma_{45}}{\sigma_{44}}\right)^{1.90} \quad (14a)$$

$$\tau_5 = 0.98 \left(\frac{\sigma_{45}}{\sigma_{44}}\right)^{2.90} \quad (14b)$$

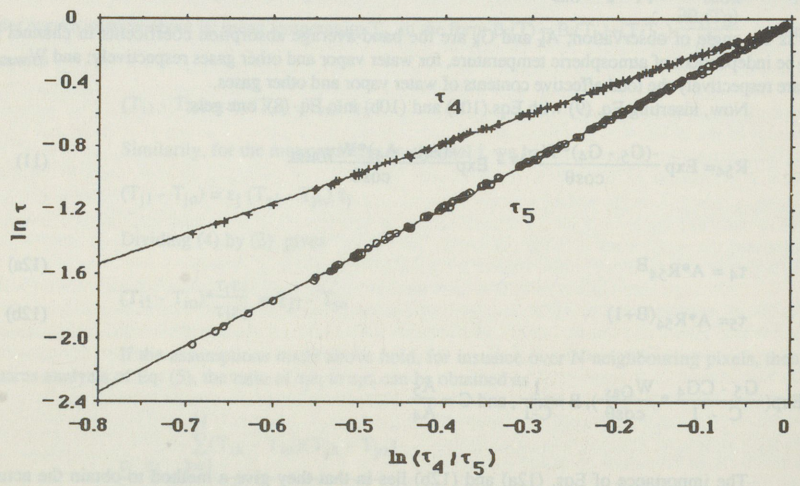


*FIGURE 1.- Logarithm of the transmittance for AVHRR Channels 4 and 5 versus the logarithm of the transmittance ratio $R_{54}$. The solid line is the linear regression of the points.*

On the other hand we plot the total column content of water vapor computed from the radiosonde data against $\cos\theta \ln R_{54}$ in Figure 2. From this figure we obtain,

$$W=0.259-14.253 \cos\theta \ln R_{54} - 11.649 (\cos\theta \ln R_{54})^2 \quad (15)$$

the relationship is clearly non linear, for AVHRR/2 data. A linear fit was also tried, but it actually gave a curvature in the residuals, that disappear when a second-order polynomial is fitted.

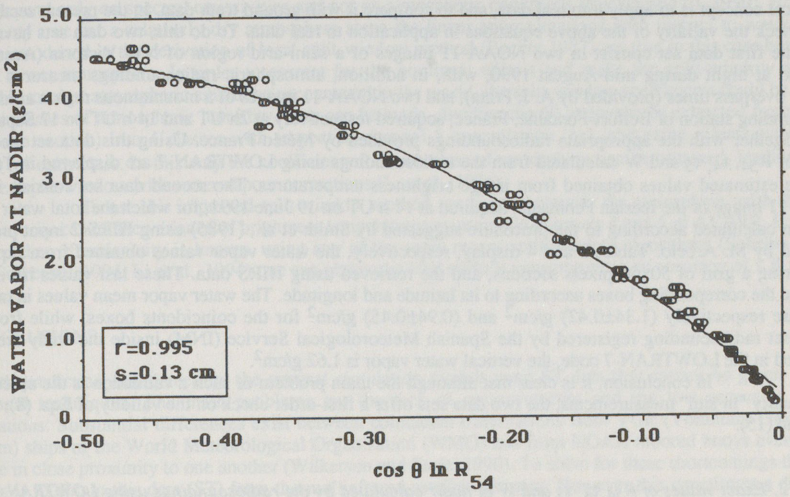


*FIGURE 2.- Total water vapor at nadir versus the modeled transmittance ratio. The correlation coefficient (r) and the standard error of estimate (s) are given in the figure. The solid line is the quadratic regression of the points.*

Now, the performance of the numerical expressions given by Eqs. (14a), (14b) and (15) is to be analyzed. To accomplish this, a new simulation using five standard atmospheres included in LOWTRAN-7 code (tropical, midlatitude summer, midlatitude winter, subartic summer, and subartic winter) has been made. The results are given in Table 1. In spite of the fact that the table includes the worst situation (an observation angle of 46°) the results corroborate the validity of the modeled transmittance and the total water vapor.

*TABLE 1.- Mean and standard deviation between the exact values of $\tau_4$, $\tau_5$ and W calculated from LOWTRAN-7 and the estimated values obtained from Eqns. (14a), (14b) and (15) using the simulated brightness temperatures in Channels 4 and 5, through $R_{45}$, as a function of several combinations of the emissivity difference, $\Delta\varepsilon=\varepsilon_4-\varepsilon_5$, over N adjacent fields of view.*

| | 46° | | | | | |
|---|---|---|---|---|---|---|
| $\Delta\varepsilon$ | $\Delta\tau_4$ | $\sigma\tau_4$ | $\Delta\tau_5$ | $\sigma\tau_5$ | $\Delta$W (cm) | $\sigma$W(cm) |
| -0.02 to0.02 | -0.013 | 0.016 | -0.010 | 0.012 | -0.039 | 0.079 |
| -0.02 to 0.01 | -0.022 | 0.026 | -0.023 | 0.028 | 0.014 | 0.066 |
| -0.02 to 0.0 | -0.031 | 0.037 | -0.035 | 0.041 | 0.064 | 0.097 |
| -0.01 to 0.01 | -0.016 | 0.019 | -0.014 | 0.017 | -0.024 | 0.068 |
| -0.01 to 0 | -0.025 | 0.029 | -0.027 | 0.032 | 0.028 | 0.070 |
| 0 | -0.017 | 0.021 | -0.016 | 0.020 | -0.016 | 0.063 |
| -0.01 | -0.034 | 0.040 | -0.039 | 0.045 | 0.078 | 0.109 |
| -0.02 | -0.047 | 0.054 | -0.056 | 0.065 | 0.150 | 0.183 |
| 0.01 | 0.004 | 0.005 | 0.011 | 0.013 | -0.130 | 0.160 |
| 0.02 | 0.028 | 0.032 | 0.043 | 0.050 | -0.266 | 0.310 |

### 3.2. Application to satellite radiometer data

In the previous subsection, the mathematical expressions derived to obtain the channel transmittances, and the total water vapor were found valid in application to simulated data. However, it is clear that the very test of any theoretical concept is to apply it to real data, and to compare it with ground truth data. In the present section we try to check the validity of the above equations in application to real data. To do this, two data sets have been used. The first data set consist in two NOAA-11 images of a semi-arid region of NW Victoria (Australia), collected at night during mid-August 1990, with, in addition, atmospheric radiosoundings measured at the satellite overpass times (provided by A. J. Prata), and two NOAA-11 images of a mountainous region around the radiosounding station of Belfort-Fontaine, France, acquired respectively at 2h UT and 14 h UT on 17 September 1992, together with the appropriate radiosoundings provided by Météo France. Using this data set the exact values of $R_{54}$, $\tau_4$, $\tau_5$ and W calculated from the radiosoundings using LOWTRAN-7 are displayed in Table 2 with the estimated values obtained from image brightness temperatures. The second data set consists in one NOAA-11 image of the Iberian Peninsule, acquired at 14 h UT on 19 June 1991, for which the total water vapor has been calculated according to the procedure suggested by Smith et al., (1985) using HIRS-2 input profiles, provided by M. Arbelo. Tables 3 and 4 display, respectively, the water vapor values obtained from Eq. (15), considering a grid of 50x50 pixels sections, and the retrieved using HIRS data. These last values have been placed in the correponding boxes according to its latitude and longitude. The water vapor mean values in tables 2 and 3 are respectively (1.34±0.42) g/cm$^2$ and (0.94±0.45) g/cm$^2$ for the coincidents boxes, while from the coincident radiosounding registered by the Spanish Meteorological Service (INM) inside the study area and processed in the LOWTRAN-7 code, the vertical water vapor is 1.62 g/cm$^2$.

In conclusion, it is clear that although the main problem of such a validation is the absence of good quality "in situ" measurements, the two data sets offer a first-order check on the validity of Eqs. (8), (14a), (14b) and (15).

*TABLE 2.-Exact values of $R_{54}$ $\tau_4$, $\tau_5$ and W at nadir calculated by the radiosoundings using LOWTRAN-7 and from Eqs. (8), (14a), (14b) and (15) using satellite brightness temperatures.*

| | AVHRR | | | | LOWTRAN-7 | | | |
|---|---|---|---|---|---|---|---|---|
| Image | $R_{54}$ | $\tau_4$ | $\tau_5$ | W | $R_{54}$ | $\tau_4$ | $\tau_5$ | W |
| NW Victoria 1 | 0.921 | 0.878 | 0.809 | 1.35 | 0.931 | 0.859 | 0.800 | 1.13 |
| NW Victoria 2 | 0.912 | 0.861 | 0.785 | 1.42 | 0.924 | 0.846 | 0.782 | 1.12 |
| Belfort (night) | 0.840 | 0.704 | 0.591 | 1.69 | 0.864 | 0.744 | 0.643 | 1.44 |
| Belfort (day) | 0.970 | 0.924 | 0.897 | 0.70 | 0.950 | 0.881 | 0.837 | 1.03 |

*TABLE 3.-a) Water vapor values along the path (Eqn. 15) for the NOAA-11 AVHRR of the Iberian Peninsula. The C values corresponding to cloudy areas.*

| | | | | | | | | | | | | | |
|---|---|---|---|---|---|---|---|---|---|---|---|---|---|
| 1.42 | 2.22 | 0.70 | 1.52 | 1.62 | 1.50 | 1.36 | 1.10 | 0.80 | 1.28 | 1.44 | 1.44 | 1.44 | 1.46 |
| 1.80 | 0.58 | 1.20 | 1.18 | 0.88 | 0.60 | 0.44 | 0.98 | 1.38 | 1.52 | 0.90 | 0.92 | 1.36 | 1.62 |
| 2.20 | 1.24 | 0.84 | C | 1.18 | 1.58 | 1.62 | 1.38 | 1.28 | 1.28 | 1.48 | 1.66 | 1.56 | 1.68 |
| 1.86 | 0.46 | 0.72 | 0.36 | 1.60 | 1.40 | 1.36 | 1.42 | 1.40 | 1.42 | 1.62 | 1.58 | 1.66 | 1.70 |
| 1.86 | 1.06 | C | C | 1.22 | 1.12 | 1.52 | 1.16 | 1.52 | 1.38 | 1.22 | 1.12 | 1.46 | 1.58 |
| 2.10 | 1.76 | 0.52 | 0.90 | 0.98 | 1.50 | 1.40 | 1.02 | 0.92 | 1.60 | 1.56 | 0.92 | 1.60 | 1.80 |
| 1.60 | 1.98 | 1.44 | 0.98 | 1.34 | 1.36 | 1.24 | 1.80 | 1.46 | 1.10 | 0.76 | 1.38 | 2.24 | 1.14 |

*TABLE 4.- Water vapor values obtained from HIRS data.*

| | | | | | | | | | | | | | |
|---|---|---|---|---|---|---|---|---|---|---|---|---|---|
| --- | 1.17 | --- | 0.64 | --- | 1.04 | --- | 0.94 | --- | --- | --- | 0.55 | 0.86 | --- |
| --- | --- | --- | --- | --- | --- | --- | --- | --- | --- | --- | 0.64 | 0.53 | --- |
| 2.52 | 0.92 | 1.56 | --- | 0.76 | --- | --- | 1.09 | 0.96 | --- | --- | --- | --- | --- |
| --- | 0.92 | --- | --- | 0.75 | --- | --- | --- | --- | --- | --- | 0.47 | --- | --- |
| --- | --- | --- | 1.06 | --- | --- | --- | --- | --- | --- | --- | --- | --- | --- |
| --- | --- | --- | --- | --- | --- | --- | 1.03 | 0.76 | --- | 0.60 | --- | --- | --- |
| --- | --- | --- | --- | --- | --- | --- | --- | --- | --- | --- | --- | --- | --- |

## 4- IMPROVING THE SPLIT-WINDOW METHOD

Based on the above results, we propose in the present section another extension of the split-window technique for land surface temperature (LST) determination that incorporates the information on the atmospheric transmittance and lead to an improved algorithm for the atmospheric correction.

As mentioned in the Introduction, the split-window approach is currently utilized to produce surface temperature retrievals in terms of a linear combination of brightness temperatures measured in AVHRR Channels 4 and 5, according to, $T_s = T_4 + \alpha (T_4 - T_5) + \beta$, where $\alpha$ and $\beta$ are the split-window coefficienst, which depend only on spectral emissivities and not on atmospheric conditions (Becker and Li, 1990). However this is only true for a relatively dry atmosphere since the linear approximations with respect to water vapor content introduced in the derivation of local split-window method (Becker 1987) are true in this case but not in case of a wet atmosphere. In order to correct for the nonlinear effects and make the split-window method applicable to most atmospheric situations encountered in the world, the split-window coefficients could be varied with the classes of atmospheric humidity. This can be made, dividing the 60 atmospheres extracted from TIGR (see above section) into 4 classes with respect to channel 5 transmission ($\tau_5$), and using a least-squares fit method for each class. In this way the coefficients for each class of atmosphere can be obtained, leading to an improved split-window with water vapour corrections (Li et al., 1994).

To use this improved split window method, we have to classify the atmosphere, with the help of the covariance and the variance of brightness temperatures measured in channels 4 and 5 of AVHRR. It should be noted that, if emissivity is known, using any of the more recent split-window algorithms (Sobrino et al., 1993; Coll et al., 1994, Li et al., 1994) one can obtain the land surface temperature to an accuracy of 1 K.

## 5-CONCLUSIONS

For both prediction and detection, the general circulation models need ST data that cannot be given by the traditional techniques. The main problems are the lack of measurements and the low accuracy of the observations. Substantial differences exist between coincident observations from VOP (Voluntary Observing Program) ships of the World Meteorological Organization (WMO) and from NOAA moored buoys even when they are in close proximity to one another (Wilkerson and Earle, 1990). To solve for these shortcomings the best solution is to obtain this data (ST) from thermal infrared satellite imagery. However this constitutes a difficult task that has been severely limited because of the difficulty in evaluating the effects of the atmosphere. The present paper should help solving this drawback through the development of a technique that permits modeling the transmittance ratio, the channel atmospheric transmittance and the total water vapor from brightness temperatures measured at Channels 4 and 5 of AVHRR on board NOAA-11 satellite alone. The technique relies on the simple condition that the atmosphere is unchanged over the neighboring points where the surface temperature and emissivity changes. This permits derive a split-window algorithm which results in an improvement over the standard algorithms for relating ST and the brightness temperatures measured by the satellite borne sensor ($T_4$ and $T_5$).

Although it is clear that even more statistics will be necessary to test the technique, the applications to real and simulated data given in this paper show that the technique is promising and could be implemented in a production environment necessary to document global climate change.


## ACKNOWLEDGMENTS

The authors wish to express their gratitude to the Laboratoire de Météorologie Dynamique (Paris, France) for supplying the TIGR data sets, and to the Air Force Geophysics Laboratory (Massachusetts, USA) for supplying the LOWTRAN-7 computer code. We also thank M. Arbelo for providing the TOVS data and C. Badenas for assistance in the processing of AVHRR data. The work was supported in part by the Commission of the European Communities (Projects No. EV5V-CT91-0033/0035).


## REFERENCES


Barton I. J., Zavody A. M., O'Brien D. M., Cutten D. R., Saunders R. W. and Llewellyn-Jones T., 1989. Theoretical algorithms for satellite-derived sea surface temperatures. J. Geophys. Res. 94: 3365-3375.

Becker F., 1987. The impact of spectral emissivity on the measurement of land surface temperature from a satellite. Int. J. Remote Sens. 8: 1509-1522.

Becker F., Li Z.-L., 1990. Towards a local split window method over land surfaces. Int. J. Remote Sens. 11: 369-394.

Chesters D., Uccellini L. W., and Robinson W. D., 1983. Low level water vapor fields from the VISSR atmospheric sounder (VAS) split-window channels. J. Climate Appl. Meteorol., 22: 725-743.

Coll C., Caselles V., Sobrino J. A., and Valor E., 1994. On the atmospheric dependence of the split-window equation for land surface temperature. Int. J. Remote Sens., (in the press).

Dalu G., 1987. Satellite remote sensing of atmospheric water vapor. Int. J. Remote Sens. 7: 1089-1097.

Deschamps P.Y., and Phulpin T., 1980. Atmospheric correction of infrared measurements of sea surface temperature using channels at 3.7, 11 and 12 μm. Bound. Layer Met. 18: 131-143.

Harris A. R., and Mason I. M., 1992. An extension to the split-window technique giving improved atmospheric correction and total water vapour. Int. J. Remote Sens. 13: 881-892.
Jedlovec G. J., 1990. Precipitable water estimation from high-resolution split-window radiance measurements. J. Appl. Meteor. 29: 863-876.
Kaufmann Y. J., and Gao B.-C., 1992. Remote sensing of water vapor in the Near IR from EOS/MODIS. IEEE Trans. Geosci. Remote Sensning. 30: 871-884.
Kleespies T.J., and McMillin L.M., 1990. Retrieval of precipitable water from observations in the split-window over varying surface temperatures. J. Appl. Meteor. 29: 851-862.
Kneizys FX, Shettle EP, Abreu LW, Anderson GP, Chetwynd JH, Gallery WO, Selby JEA, Clough SA (1988) Users guide to LOWTRAN 7. Technical Report AFGL-TR-88-0177, Optical/Infrared Technology Division, U.S. Air Force Geophysics Laboratory, Hascom Air Force Base, Massachusetts.
Li Z.-L., Becker F., Stoll M. P., and Sobrino J. A., 1994. Intercomparison of an improved local split window with other split window algorithms for estimating land surface temperature from AVHRR data. J. Geophys. Res. (submitted).
McClain EP, Pichel WG, Walton CC (1985) Comparative performance of AVHRR-Based multichannel sea surface temperatures. J. Geophysical Res. 90: 11,587-11,601.
McMillin L. M ., 1975. Estimation of sea surface temperature from two infrared window measurements with different absorption. J. Geophys. Res. 80: 5113-5117.
Prabhakara C, Dalu G, Lo R.C., and Nath, N.R., 1979. Remote sensing of seasonal distribution of precipitable water vapor over the oceans and the inference of boundary-layer structure. Mon. Weather Rev., 107: 1388-1401.
Price J. C., 1984. Land surface temperature measurements from the split window channels of the NOAA 7 AVHRR. J. Geophys. Res. D5: 7231-7237.
Schluessel P., 1989. Satellite derived low level atmospheric water vapor content from synergy of AVHRR with HIRS. Int. J. Remote Sens. 10: 705-721.
Scott N. A., and Chedin A., 1981. A fast line by line method for atmospheric absorption computations: The Automatized Atmospheric Absorption Atlas. J. Appl. Meteorol. 20: 802-812.
Smith W. L. et al., 1985. The simultaneous retrieval export package. Second International TOVS Study Conference. Feb. 18-22, Igls, pp. 224-253.
Sobrino, J. A., Coll C., and Caselles V., 1991. Atmospheric correction for land surface temperature using NOAA-11 AVHRR Channels 4 and 5. Remote Sens. Environ. 38: 19-34.
Sobrino, J. A., Caselles V., and Coll C., 1993. Theoretical split-window algorithms for determining the actual surface temperature. Il Nuovo Cimento. 16:219-236.
Sobrino, J. A., Z.-L., Li, and Stoll M.P., 1994. Imact of the atmospheric transmittance and total water vapor content in the algorithms for estimating sateliite sea surface temperaturs. IEEE Trans. Geosci. Remote Sensing, (in press).
Sobrino, J. A., Z.-L., Li, Stoll M.P. and F. Becker, 1994. Improvements in the split-window technique for land surface temperature determination. IEEE Trans. Geosci. Remote Sensing, (in press).
Wilkerson J. C., and Earle M. D., 1990. A study of differences between environmental reports by ships in the voluntary observing program and measurements from NOAA buoys. J. Geophys. Res. 95: 3373-3385.